ISSN 1674-1056
http://cpb.iphy.ac.cn
http://iopscience.iop.org/cpb
中国物理 B
Chinese Physics
中国物理
Chinese Physics B

Improvement of electro-optic performances in white organic light emitting diodes with color stability by buffer layer and multiple dopants structure

Zhi-Qi Kou(寇志起), Yu Tang(唐宇), Li-Ping Yang(杨丽萍), Fei-Yu Yang(杨飞宇), Wen-Jun Guo(郭文军)

Citation: Chin. Phys. B . 2018, 27(10): 107801. **doi:** 10.1088/1674-1056/27/10/107801

Journal homepage: http://cpb.iphy.ac.cn; http://iopscience.iop.org/cpb

What follows is a list of articles you may be interested in

Characteristic improvements of thin film AlGaInP red light emitting diodes on a metallic substrate

Bin Zhao(赵斌), Wei Hu(胡巍), Xian-Sheng Tang(唐先胜), Wen-Xue Huo(霍雯雪), Li-Li Han(韩丽丽), Ming-Long Zhao(赵明龙), Zi-Guang Ma(马紫光), Wen-Xin Wang(王文新), Hai-Qiang Jia(贾海强), Hong Chen(陈弘)
Chin. Phys. B . 2018, 27(4): 047803. **doi:** 10.1088/1674-1056/27/4/047803

High color rendering index white organic light-emitting diode using levofloxacin as blue emitter

Miao Yan-Qin, Gao Zhi-Xiang, Zhang Ai-Qin, Li Yuan-Hao, Wang Hua, Jia Hu-Sheng, Liu Xu-Guang, Tsuboi Taiju
Chin. Phys. B . 2015, 24(5): 057802. **doi:** 10.1088/1674-1056/24/5/057802

Improvement of electron injection of organic light-emitting devices by inserting a thin aluminum layer into cesium carbonate injection layer

Xin Li-Wen, Wu Xiao-Ming, Hua Yu-Lin, Xiao Zhi-Hui, Wang Li, Zhang Xin, Yin Shou-Gen
Chin. Phys. B . 2015, 24(3): 037802. **doi:** 10.1088/1674-1056/24/3/037802

Effect of NaCl doped into Bphen layer on the performance of tandem organic light-emitting diodes

Xiao Zhi-Hui, Wu Xiao-Ming, Hua Yu-Lin, Bi Wen-Tao, Wang Li, Zhang Xin, Xin Li-Wen, Yin Shou-Gen
Chin. Phys. B . 2014, 23(8): 087811. **doi:** 10.1088/1674-1056/23/8/087811

Pure blue and white light electroluminescence in a multilayer organic light-emitting diode using a new blue emitter

Wei Na, Guo Kun-Ping, Zhou Peng-Chao, Yu Jian-Ning, Wei Bin, Zhang Jian-Hua
Chin. Phys. B . 2014, 23(7): 077802. **doi:** 10.1088/1674-1056/23/7/077802

Improvement of electro-optic performances in white organic light emitting diodes with color stability by buffer layer and multiple dopants structure

Zhi-Qi Kou(寇志起)†, Yu Tang(唐宇), Li-Ping Yang(杨丽萍), Fei-Yu Yang(杨飞宇), and Wen-Jun Guo(郭文军)

College of Science, University of Shanghai for Science and Technology, Shanghai 200093, *China*

(Received 23 May 2018; revised manuscript received 6 July 2018; published online 10 September 2018)

A series of white phosphorescent OLED devices with buffer layer and multiple dopant structure is investigated in order to obtain better electro-optic performances and color stability. The color coordinate and color stability are related to the location of multiple dopants layer, and the optimized location can compensate for the change of the blue emission intensity under a high voltage and stabilize the spectrum. The electro-optic performances and color stability can be further improved by changing the composition and thickness of the buffer layer between the emitting layer and the electron transport layer. In device B2, the distance from multiple dopant layer to buffer layer is 2 nm and the thickness of buffer layer is 5 nm, the maximum luminance, current density, and power efficiency can reach 9091 cd/m^2, 364.5 mA/cm^2, and 26.74 lm/W, respectively. The variation of international commission on the illumination (CIE) coordinate of device B2 with voltage increasing from 4 V to 7 V is only (0.006, 0.004).

Keywords: organic light emitting diodes, multiple dopants layer, buffer layer, color stability

PACS: 78.60.Fi, 85.60.jb, 73.21.Ac **DOI:** 10.1088/1674-1056/27/10/107801

1. Introduction

White organic light emitting diodes (WOLEDs) have attracted tremendous attention for their many applications in full-color flat-panel displays and solid state lighting, due to their advantages including light weight, high resolution, flexibility, and large area back light.[1–3] In order to meet the wider commercial applications, WOLEDs with high efficiency, low cost, and high color stability are prerequisite.[4,5]

In the past two decades, WOLEDs have been significantly developed by various approaches, including new material innovation and device structure optimization and so on. The phosphorescent materials are often used as emitters because they can harvest both singlet and triplet excitons and achieve an internal quantum efficiency of 100% in principle.[6] In WOLED devices, three primary or two complementary colors' emitters are usually incorporated and distributed in the emitting layer (EML).[7,8] For higher performance WOLEDs, many device structures have been reported. Although the undoped WOLED device has advantages of simple structure and low cost, the efficiency and efficiency roll-off become worse due to a severe concentration quenching effect.[9–11] Color stable and high efficient WOLEDs with doping structure are usually based on two kinds of device structures, including a single emitting layer with multiple dopants (SEML-MD),[12] and a multiple emitting layer with single dopant (MEML-SD).[13–16] Kim *et al.* realized a high performance single emitting layer with three color dopant WOLED with a maximum luminance of 37810 cd/m^2 at 11 V and a luminous efficiency of 48.10 cd/A at 5 V,[12] but the emission is not stable with increasing driving voltage and it is not easy to precisely control the doping process for optimum doping concentration ratio among three dopants.[17] For the MEML-SD WOLED device, Chen and Han reported color-stable WOLED devices by using the mixed-host EML structure, which can alleviate the shift of recombination zone and obtain better charge balance, but CIE (1931) coordinates of their devices are far from the white light region.[13,14] Liu *et al.* achieved a pure white OLED device with CIE coordinate of (0.33, 0.38) at a luminance of 10000 cd/m^2 by using a hybrid emitting structure, but the device shows a poor color stability, the CIE coordinate changes from (0.50, 0.42) to (0.33, 0.38) with the increase of luminance from 10 cd/m^2 to 10000 cd/m^2.[15] Hence, high efficiency and color stability WOLEDs with simplified structure and easy fabrication should be further studied.

In this paper, we fabricate a series of white phosphorescent OLED devices with multiple emitting layers with multiple dopant (MEML-MD) structure and buffer layer between EML and electron transport layer (ETL). The MEML is comprised of single dopant (FIrpic) EML and multiple dopants EML (FIrpic: PO-01). Compared with the three-dopant EML device, the two-dopant EML device has the fabrication process that is easy to control. The location of multiple-dopant EML can affect the CIE coordinate. The buffer layers are formed by mixing electron transport material (TPBi) and hole transport material (TCTA) with different ratios. Different carrier transport properties of TPBi and TCTA will affect the carrier

†Corresponding author. E-mail: usst102@aliyun.com

© 2018 Chinese Physical Society and IOP Publishing Ltd

injection balance, and then influence the recombination zone extension and color stability.[18] We achieve high performance WOLEDs with pure white emitting and superior color stability by adjusting the location of multiple dopants in EML and mixed ratio of TPBi in the buffer layer.

2. Experiment

Prior to the deposition of organic layers, the substrates with indium tin-oxide (ITO) were cleaned by ultrasonic bath for 15 min in each of the following processes: detergent, deionized water, isopropyl alcohol. All layers were grown by thermal evaporation at a base pressure of $< 5 \times 10^{-5}$ Pa without breaking the vacuum. The host materials were grown on the substrates at a rate of 1 Å/s, and the dopant and mixed host were both grown at a rate of 2 Å/s. The current density, luminance, efficiency, and electroluminescence (EL) spectrum were obtained using a Keithley 2400 digital power and a PR655 spectrometer.

In all of the devices, the iridium-bis-(4,6,-difluorophenyl-pyridinato-N,E)-picolinate (FIrpic) was used as blue dopant and the iridium(III) bis (4-phenylthieno[3,2-c] pyridinato-0 N,E) acetylace- tonate (PO-01) was used as orange dopant. The concentration ratios of FIrpic and PO-01 were fixed at 8% and 1%, respectively. The host material in EML was 4,4',4'-tris(Ncarbazolyl) triph- enylamine (TCTA). The buffer layer was a mixture of TCTA and 2, 2',2"-(1,3,5-benzinetriyl)-tris(1-phenyl-1-H-benzimidazole) (TPBi) in a certain proportion. The 1, 1-bis (di-4-tolylaminophe-nyl) cyclohexane (TAPC) and 1,3,5-tri (m-pyrid-3-ylphenyl) benzene (TmPyPB) were chosen as the hole transport layer (HTL) and ETL. The hole injection layer (HIL) and electron injection layer (EIL) were of 1,4,5,8,9,11-hexaazatriphenylene-hexacarbonitrile (HAT-CN) and 8-hydroxyquinolinolato lithium (Liq), respectively. The basic structures of devices are as follows: ITO (100 nm)/HAT-CN (10 nm)/TAPC (40 nm)/TCTA: 8%FIrpic ((10-x) nm)/TCTA: 1%PO-01: 8%FIrpic (5 nm)/TCTA: 8%FIrpic (x nm)/TCTA$_{1-y}$: TPBi$_y$ (5 nm)/TmPyPB (30 nm)/Liq (2 nm)/Al (100 nm). The detailed structures of EML and buffer layer are listed in Table 1. The basic structure diagram and energy level diagram of WOLEDs are shown in Fig. 1. The energy levels of organic materials are obtained from Refs. [19] and [20].

Table 1. Detailed structures of EMLs and buffer layers.

Device	EML 1	EML 2	EML 3	Buffer layer
A1	TCTA: 8%FIrpic(10 nm)	TCTA: 1%PO-01: 8%FIrpic(5 nm)		
A2	TCTA: 8%FIrpic(10 nm)	TCTA: 1%PO-01: 8%FIrpic(5 nm)		1/2TCTA: 1/2TPBi(5 nm)
A3	TCTA: 8%FIrpic(8 nm)	TCTA: 1%PO-01: 8%FIrpic(5 nm)	TCTA: 8%FIrpic(2 nm)	1/2TCTA: 1/2TPBi(5 nm)
A4	TCTA: 8%FIrpic(6 nm)	TCTA: 1%PO-01: 8%FIrpic(5 nm)	TCTA: 8%FIrpic(4 nm)	1/2TCTA: 1/2TPBi(5 nm)
B1	TCTA: 8%FIrpic(8 nm)	TCTA: 1%PO-01: 8%FIrpic(5 nm)	TCTA: 8%FIrpic(2 nm)	1/4TCTA: 3/4TPBi(5 nm)
B2	TCTA: 8%FIrpic(8 nm)	TCTA: 1%PO-01: 8%FIrpic(5 nm)	TCTA: 8%FIrpic(2 nm)	TPBi(5 nm)
C1	TCTA: 8%FIrpic(8 nm)	TCTA: 1%PO-01: 8%FIrpic(5 nm)	TCTA: 8%FIrpic(2 nm)	1/2TCTA: 1/2TPBi(2 nm)

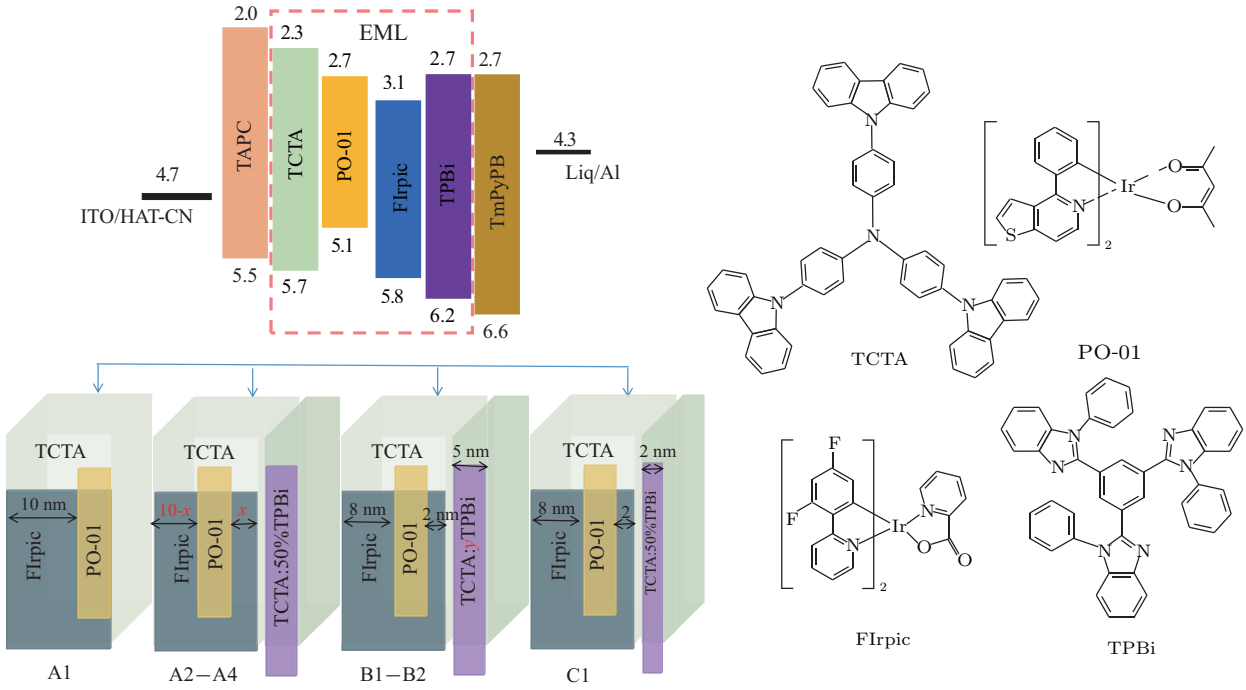


Fig. 1. (color online) Schematic diagrams of energy level and EML in devices A, B, and C with insert showing molecular structures of partial materials.

3. Results and discussion

Firstly, we fabricate a series of devices A1, A2, A3, and A4 as shown in Fig. 1 in order to investigate the influence of the buffer layer and location of multiple-dopant EML. There is no buffer layer in device A1, the mixed ratio between TPBi and TCTA in the buffer layer is 1:1 in each of devices A2, A3, and A4. Table 2 lists the EL characteristic values of the devices tested with different structures.

Table 2. EL characteristics of devices tested with different structures.

Device	Luminance L_{max}/(cd/m^2)	CD[a]/(mA/cm^2)	PE[b]/(lm/W)	CE[c]/(cd/A)	CIE (1931)		
					4 V	5.5 V	7 V
A1	17310	197.2	69.66	60.98	(0.446, 0.492)	(0.428, 0.487)	(0.413, 0.483)
A2	10120	292.7	34.67	30.35	(0.429, 0.464)	(0.404, 0.447)	(0.352, 0.401)
A3	7531	263.7	24.33	21.30	(0.303, 0.429)	(0.303, 0.412)	(0.296, 0.404)
A4	5628	274.0	16.80	14.71	(0.236, 0.388)	(0.251, 0.382)	(0.254, 0.353)
B1	8524	407.1	23.80	20.83	(0.306, 0.440)	(0.306, 0.433)	(0.300, 0.418)
B2	9091	364.5	26.74	23.40	(0.330, 0.460)	(0.330, 0.459)	(0.324, 0.456)
C1	8504	212.6	57.89	50.67	(0.328, 0.459)	(0.321, 0.453)	(0.311, 0.440)

[a]CD is the current density. [b]PE is the power efficiency. [c]CE is the current efficiency.

Figure 2(a) shows the curves of luminance and current density versus voltage of devices A1–A4. The maximum luminance values of devices A1, A2, A3, and A4 are 17310 cd/m^2, 10120 cd/m^2, 7531 cd/m^2, and 5628 cd/m^2, respectively. Because TPBi is a well-known electron transport material with an electron mobility of 3.3×10^{-5} cm^2/V·s,[20] it can enhance the capability of electron injection. At the same time, the lowest unoccupied molecular orbital (LUMO) level of TPBi (−2.7 eV) is equal to that of TmPyPB, and the TCTA in the buffer layer is the same as the host material in the EML, the buffer layer is beneficial to the improvement of the injection capacity of electrons. So the current densities of devices A2, A3, and A4 are similar to each other, which are all larger than that of device A1.

Figure 2(b) shows curves of current efficiency and power efficiency versus current density of devices A1, A2, A3, and A4. The maximum current efficiency values of devices A1, A2, A3, and A4 are 60.98 cd/A, 30.35 cd/A, 21.30 cd/A, and 14.71 cd/A, corresponding to the maximum power efficiency values of 69.66 lm/W, 34.67 lm/W, 24.33 lm/W, and 16.80 lm/W. Although the efficiency of device A1 is largest, the efficiency roll-off is also the most serious in four devices. The reason is that the recombination zone (RZ) of device A1 without buffer layer, which can improve the electron injection and expand RZ, is narrowest. The efficiency gradually decreases with multiple-dopant layer moving from ETL to HTL because the utilization of PO-01 material gradually decreases. The TCTA is a typical hole transport host material, which will lead the RZ to approach to the interface between EML and ETL and the width of RZ is approximately 3 nm.[21] The triplet energy of PO-01 (2.21 eV) is lower than that of FIrpic (2.60 eV), which leads to a better utilization of exciton in EML when the multiple-dopant layer is located in RZ.[22] When the multiple-dopant layer moves away from ETL, the efficiency gradually declines from device A2 to device A4. At the same time, the intensity of orange emission also decreases under the voltage of 6 V because EML2 deviates from RZ as shown in Fig. 3, in which each of all spectra contains two primary emission peaks at 472 nm and 560 nm originating from FIrpic and PO-01 respectively.

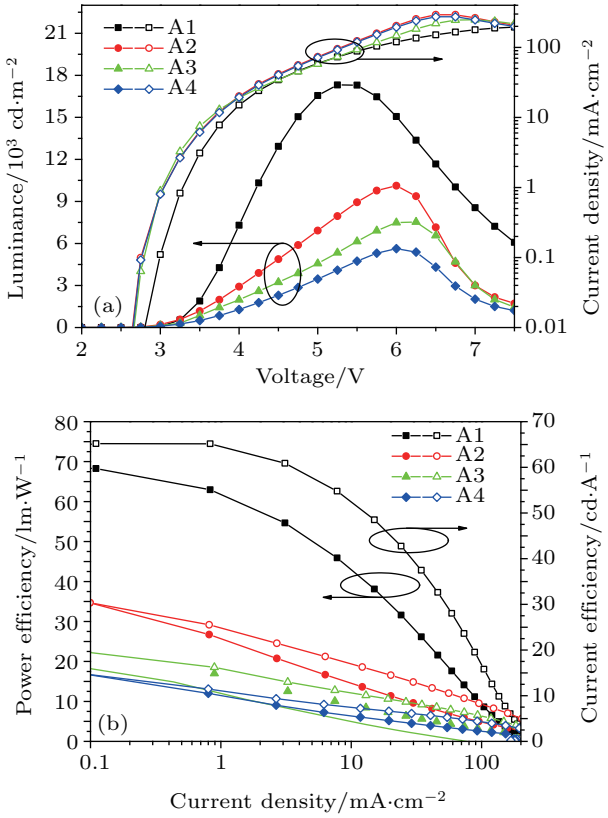


Fig. 2. (color online) (a) Curves of current density and luminance versus voltage of devices A1–A4 and (b) plots of power efficiency and current efficiency versus current density of devices A1–A4.

Figure 4 shows the normalized EL spectra and CIE coordinates of devices A1, A2, A3, and A4 at voltages ranging from 4 V to 7 V. Each of all spectra contains two primary

emission peaks at 472 nm and 560 nm originating from FIrpic and PO-01 respectively. In Figs. 4(a) and 4(b), it can be seen that the intensity of orange emission is not only higher than that of blue emission but also always at saturation state, which indicates the multiple-dopant layer is within RZ and the orange emission is dominant. Because the quantity of exciton increases, the intensity of blue emission increases with the increase of voltage. The intensity of blue emission in device A2 is also higher than that of device A1 under the same voltage because the buffer layer can expand the RZ and improve the blue emission. However, neither CIE coordinates nor color stability is better in device A1 or device A2. By moving the multiple-dopant layer toward HTL, we find that the intensity of blue emission is greatly enhanced, as shown in Figs. 4(c) and 4(d). We achieve better CIE coordinates and color stability in device A3, the CIE coordinate shifting is only (0.019, 0.045) from 4 V to 7 V. In device A4, CIE coordinates and color stability begin to deteriorate again because the multiple-dopant layer deviates far from RZ, which leads the intensity of orange emission to decrease rapidly.

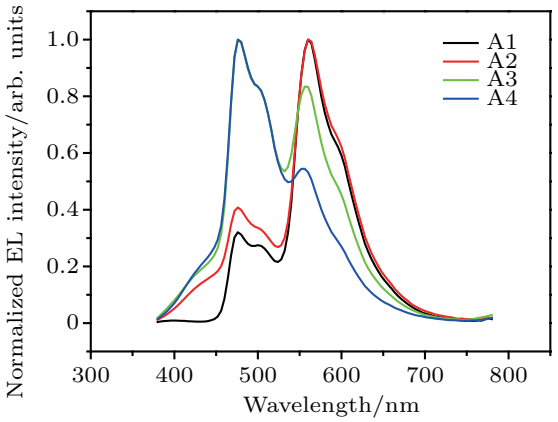


Fig. 3. (color online) Normalized EL spectra of the devices A1–A4 at the voltage of 6 V.

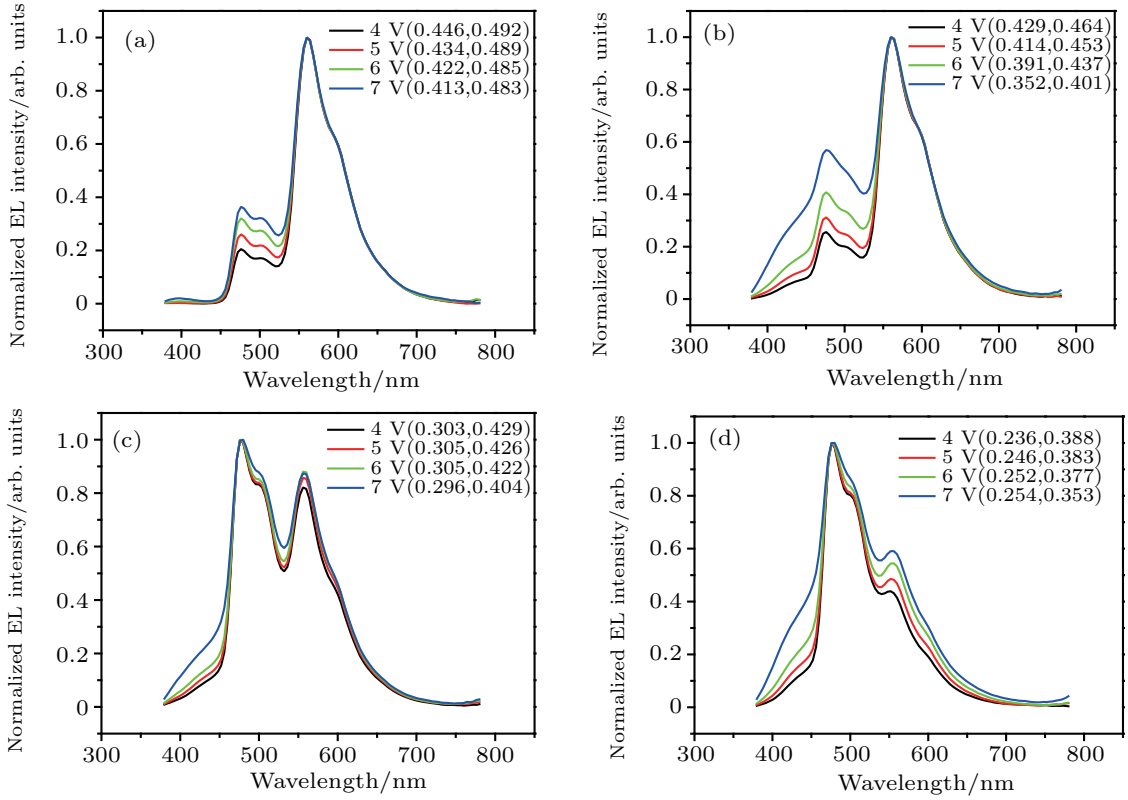


Fig. 4. (color online) Normalized EL spectra and CIE coordinates of devices (a) A1, (b) A2, (c) A3, and (d) A4 at different voltages.

Furthermore, we fabricate other devices B1, B2, and C1 on the basis of device A3 in order to improve performances of device. In devices B1 and B2, their current density and color stability are further improved by increasing the mixing ratio of TPBi in the buffer layer to 1:3 and 0:1, respectively. In device C1, its current and power efficiency are further improved by reducing the thickness of buffer layer to 2 nm.

The electro-optical characteristic curves of devices A3, B1, B2, and C1 are shown in Fig. 5 and the data are listed in Table 2. The maximum current density of device B1 is 407.1 mA/cm^2, which is the highest in these four devices. As mentioned above, the buffer layer is beneficial to the improvement of the injection capacity of electrons. When the mixing ratio of TPBi is 1:3 in the buffer layer, the current density reaches the maximum value. When the mixing ratio of TPBi in the buffer layer is above 1:3, the current density begins to decrease because of the blocking effect of TPBi on holes transport. Although the current density of device B2 is

less than that of device B1, the power and current efficiency are greater, and they are 26.74 lm/W and 23.40 cd/A, respectively. So the maximum luminance can reach to 9091 cd/m^2 in device B2 by increasing the mixing ratio of TPBi in the buffer layer to 0:1. Although the maximum current density of device C1 is 212.6 mA/cm^2 with reducing the buffer layer thickness, which is the lowest among these four devices, the power and current efficiency are the highest, which are 57.89 lm/W and 50.67 cd/A, respectively. At the same time, the maximum luminance can also reach to 8504 cd/m^2 in device C1 in the case of color stability. Under the voltage of 6 V, the normalized EL spectra and CIE coordinates of devices A3, B1, B2, and C1 are similar due to the same structure as shown in Fig. 6(a).

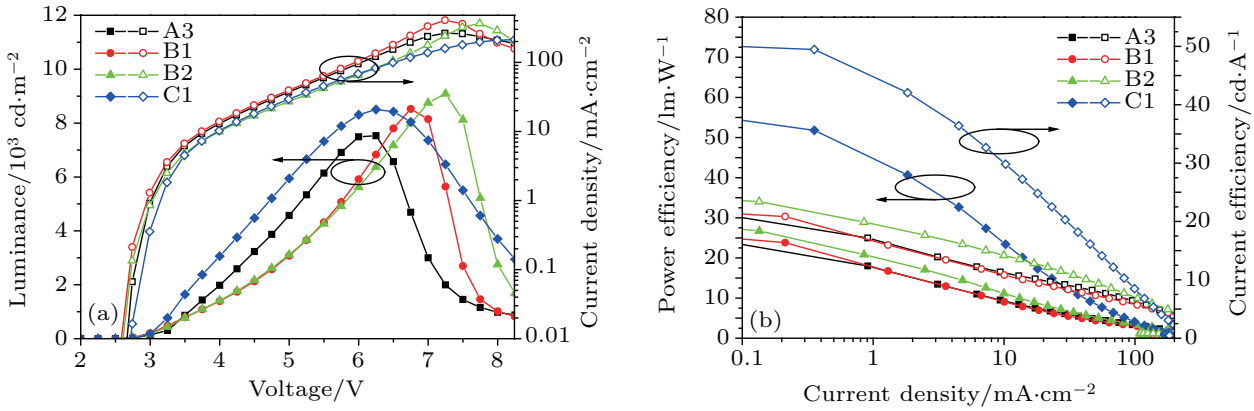


Fig. 5. (color online) (a) Curves of current density and luminance versus voltage of devices A3, B1, B2, and C1 and (b) curves of power efficiency and current efficiency versus current density of devices A3, B1, B2, and C1.

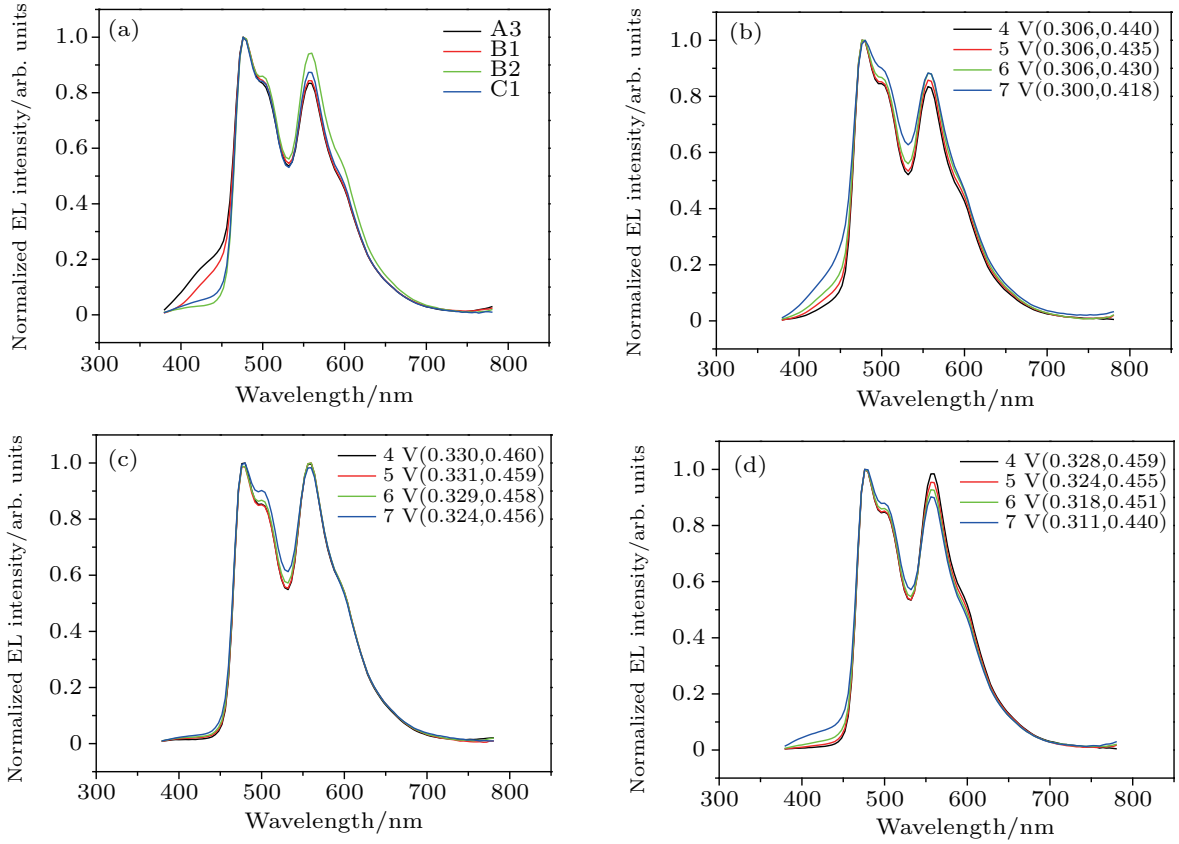


Fig. 6. (color online) (a) Normalized EL spectra of the devices A3, B1, B2, and C1 at voltage 6 V and ((b)–(d)) normalized EL spectra and CIE coordinates of devices B1, B2, and C1 at different voltages, respectively.

Figures 6(b)–6(d) show the normalized EL spectra and CIE coordinates of devices B1, B2, and C1 at voltages ranging from 4 V to 7 V. The RZ will be expanded with increasing TPBi mixed ratio in the buffer layer due to the fact that the TPBi is a typical electron transport material, which can enhance the intensity of orange emission as shown in Figs. 6(b) and 6(c). In device B2, the CIE coordinate and color stability are further improved compared with those in device A3.

The CIE coordinate of device B2 shows little variation from (0.330, 0.460) to (0.324, 0.456) with increasing the voltage from 4 V to 7 V, as shown in Fig. 7. On the contrary, the RZ will be compressed with buffer layer thickness decreasing due to the reduced electron injection capacity as shown in Fig. 6(d), which leads the intensity of orange emission to become unstable with voltage changing. The CIE coordinate of device C1 shows a slightly shifted range from (0.328, 0.459) to (0.311, 0.440) with the voltage increasing from 4 V to 7 V, as shown in Fig. 7. Device B1 exhibits a cold white spectrum similar to device A3, while device B2 and device C1 show pure white emissions.

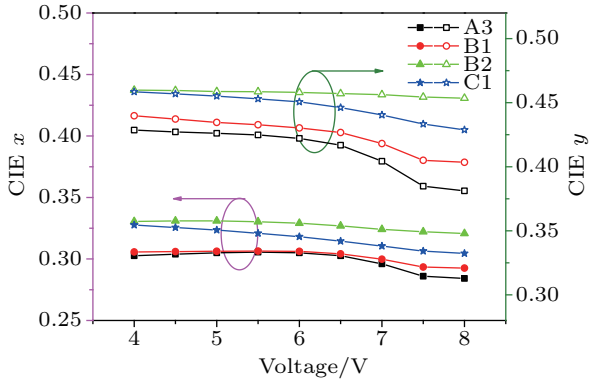


Fig. 7. (color online) Curves of CIE x and CIE y coordinates versus voltage of devices A3, B1, B2, and C1.

Besides, we note that there is an extra peak near 410 nm in EL spectra in each of devices A2, A3, A4, B1, and C1 as shown in Figs. 4 and 6. Du reported that peak wavelength in the PL spectrum of TPBi is 410 nm.[23] Because the values of triplet energy (E_T) of FIrpic and TPBi (2.6 eV) are the same, the resonant triplet energies can make the triplet excitons freely move between EML and buffer layer.[24,25] In device B2, the RZ is far from the buffer layer due to the larger TPBi mixing ratio (0:1), so there is no extra peak in device A1 without the buffer layer or B2. All of these indicate that the extra peak at 410 nm originates from TPBi.

4. Conclusions

In summary, the high efficiency and color stability WOLED are prerequisite for wider commercial applications. Firstly, the CIE coordinates and color stability are investigated by optimizing the location of multiple-dopant layer, which can compensate for the blue emission intensity under a high voltage and stabilize the spectrum. When the distance (x) from the multiple-dopant layer to the buffer layer is 2 nm, the maximum luminance, current density, and power efficiency of device A3 with stable spectra can reach 7531 cd/m^2, 263.7 mA/cm^2, and 24.33 lm/W, respectively. Secondly, the electro-optic performances and color stability can be further improved by changing the composition and thickness of the buffer layer in the case of spectral stability. The maximum luminance and current density can reach 9091 cd/m^2 and 364.5 mA/cm^2 in device B2 as the mixed ratio of TPBi reaches 0:1, the maximum power efficiency can arrive at 57.89 lm/W in device C1 as the thickness of buffer layer is 2 nm. The variation of the CIE coordinate in device B2 is only (0.006, 0.004) with the voltage increasing from 4 V to 7 V.

References

[1] Liao Y J, Lou Y H, Wang Z K and Liao L S 2014 *Chin. Phys. B* **23** 118508
[2] Ying L, Ho C L, Wu H B, Cao Y and Wong W Y 2014 *Adv. Mater.* **26** 2459
[3] Zhu W, Yu J, Qian B, Xiao T, Zhai G and Wei B 2016 *Synth. Met.* **220** 621
[4] Zhu Y K, Zhong J, Lei S Y, Chen H, Shao S S and Lin Y 2017 *Chin. Phys. B* **26** 087302
[5] Shi X B, Gao C H, Zhou D Y, Qian M, Wang Z K and Liao L S 2012 *Appl. Phys. Express* **5** 102102
[6] Xu L, Tang C W and Rothberg L J 2016 *Org. Electron.* **32** 54
[7] Sun N, Wang Q, ZhaoY, Chen Y, Yang D, Zhao F, Chen J and Ma D 2014 *Adv. Mater.* **26** 1617
[8] Chen P, Zhao L, Duan Y, Zhao Y, Xie W, Xie G, Liu S, Zhang L and Li B 2011 *J. Lumin.* **131** 2144
[9] Islam A, Zhang D, Peng R, Yang R J, Hong L, Song W, Wei Q, Duan L and Ge Z Y 2017 *Chem. Asian. J.* **12** 2189
[10] Xue K, Han G, Duan Y, Chen P, Yang Y Q, Yang D, Duan Y H, Wang X and Zhao Y 2015 *Org. Electron.* **18** 84
[11] Ma Z, Yu J, Li L and Jiang Y D 2012 *Displays* **33** 42
[12] Kim J W, You S, Yoon N A, Cheah K W, Zhu F R and Kim W Y 2015 *Sci. Rep.* **4** 7009
[13] Chen P, Chen B, Zuo L, Duan Y, Han G, Sheng R, Xue K and Zhao Y 2016 *Org. Electron.* **31** 136
[14] Han G, Chen B, Zuo L, Xue K, Chen P, Duan Y and Zhao Y 2016 *Org. Electron.* **37** 207
[15] Liu B, Luo D, Gao D, Wang X, Xu M, Zou J, Ning H, Wang L, Peng J and Cao Y 2015 *Org. Electron.* **27** 29
[16] Wei N, Guo K P, Zhou P C, Yu J N, Wei B and Zhang J H 2014 *Chin. Phys. B* **23** 077802
[17] Qi Y, Wang Z, Hou S and Yu J 2017 *Org. Electron.* **43** 112
[18] Yang H J, Lee H W, Lee S E, Sun Y, Hwang K M, Yoo K H, Lee S K, Kim W Y and Kim Y K 2015 *Thin Solid Films* **587** 61
[19] Song W and Lee J Y 2015 *J. Phys. D: Appl. Phys.* **48** 365106
[20] Jou J H, Kumar S, Agrawal A, Li T H and Sahoo S 2015 *J. Mater. Chem.* **3** 2974
[21] Zhang H, Yang X, Cheng J, Li D, Chen H, Yu J and Li L 2017 *Org. Electron.* **50** 147
[22] Xue K, Sheng R, Duan Y, Chen P, Chen B, Wang X, Duan Y and Zhao Y 2015 *Org. Electron.* **26** 451
[23] Du Q, Wang W, Li S, Zhang D, Li W and Zheng W 2016 *Opt. Commun.* **366** 253
[24] Reineke S, Lindner F, Schwartz G, Seidler N, Walzer K, Lussem B and Leo K 2009 *Nature* **459** 234
[25] Tan T, Ouyang S, Xie Y, Wang D, Zhu D, Xu X and Fong H H 2015 *Org. Electron.* **25** 232